



Modeling acoustic resonators: From theory to application

Matthew F. Calton^{a)}

Scott D. Sommerfeldt^{b)}

Department of Physics and Astronomy, Brigham Young University

Eyring Science Center

Provo UT 84602

Acoustic resonators, such as the Helmholtz and quarter-wave resonator, can be used to attenuate unwanted noise in a space. Classical formulations can be used to approximate resonator performance for a given resonator configuration, but may lack sufficient accuracy for some applications. More detailed expressions exist, but these models may be difficult for practical implementation due to their complexity. This research aims to fully characterize the response of resonator arrays in one dimension using impedance translation and junction impedances. Then, the most concise description of the system is found by retaining the most important acoustic effects without sacrificing accuracy. This model is then compared to both simple and complex models, as well as measured data from physical resonator arrays. The modeled results for the concise description agree favorably with the measured results.

1 INTRODUCTION

Acoustic resonators are commonly used in noise control engineering where relatively simple, robust solutions are desired. Acoustic resonators typically absorb over a very small bandwidth, but are frequently used in applications where noise is constant and tonal. For example, a car muffler attenuates noise from the engine and is relatively simple and stable. Bass traps are also commonly used in concert halls to absorb certain resonances in the hall.

^{a)} email: matthewcalton@byu.edu

^{b)} email: scott_sommerfeldt@byu.edu

While there are many types of acoustic resonators, the two most common are the Helmholtz resonator and the quarter-wave tube. The Helmholtz resonator consists of a neck backed by a larger cavity (see Fig. 1a). The quarter-wave tube is a simple pipe that is open on one end and closed at the other (see Fig. 1b).

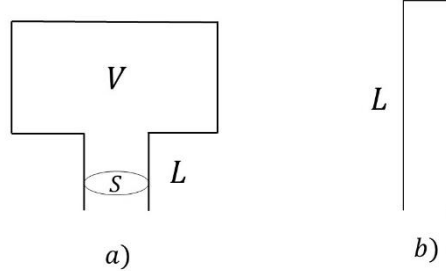


Fig. 1 - A simple representation of a) a Helmholtz resonator and b) a quarter-wave tube.

In modeling acoustic resonators, their response is often predicted by simple, low-frequency approximations that can yield significant error¹. Conversely, complicated expressions may add accuracy and detail, albeit at the cost of time and resources. This paper presents various methods for determining the response of acoustic resonators and arrays of resonators. Suggestions are given for choosing between methods.

2 THEORY

2.1 IMPEDANCE TRANSLATION METHOD

One of the most detailed methods for determining the response of acoustic resonators presented here utilizes impedance translation and waveguide circuits. The impedance translation theorem allows a given impedance to be translated over a distance in order to obtain the impedance at another point in space. The impedance translation theorem is given mathematically as follows:

$$Z_{A0} = \frac{\rho_0 c}{S} \frac{\frac{Z_{AL}}{\rho_0 c/S} + j \tan(kL)}{1 + j \frac{Z_{AL}}{\rho_0 c/S} \tan(kL)}, \quad (1)$$

where $k = \omega/c$, ρ_0 is the density of air, c is sound speed, S is the cross-sectional area of the enclosure, L is the length of translation, Z_{AL} is the acoustic impedance before the translation, and Z_{A0} is the input acoustic impedance looking into the system.

In the case of an acoustic resonator or array of resonators, many successive translations will occur over different lengths and cross-sectional areas. Therefore, it is convenient to use a circuit representation of the impedance translation theorem. Figure 2 shows the T-network (often called the waveguide circuit) that accomplishes this. For acoustic resonators such as the Helmholtz resonator, each element can be modeled as a waveguide circuit with the appropriate length and cross-sectional area. After the T-networks and junction impedances have been arranged to reflect the nature of the physical system, parameters such as acoustic impedance can be found at any point in the circuit. Since the waveguide circuit is based on the impedance translation theorem, all wave effects are preserved throughout the calculations.

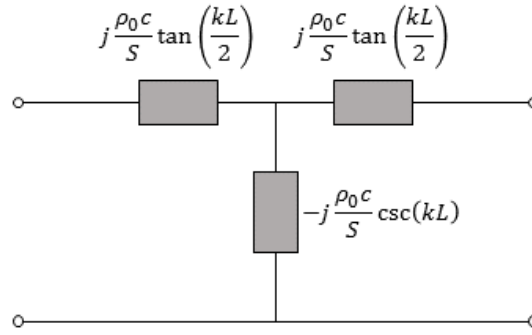


Fig. 2 - T-network representing the impedance translation theorem over a distance L with cross-sectional area S .

End corrections are accounted for by adding a corrective element between discontinuities. For concentric pipes of circular cross section, Karal² suggested a junction impedance of the following form:

$$Z_{AJ} = j\omega M_{AJ}$$

$$M_{AJ} = \frac{8\rho_0}{3\pi^2 a_1} H\left(\frac{a_1}{a_2}\right) \quad (2)$$

$$H\left(\frac{a_1}{a_2}\right) = \frac{3\pi}{2} \sum_{m=1}^{\infty} \frac{J_1^2\left(\gamma_m \frac{a_1}{a_2}\right)}{\gamma_m \frac{a_1}{a_2} [\gamma_m J_0(\gamma_m)]^2}$$

In Eqn. (2), a_1 and a_2 are the radii of the adjoining pipes, γ_m is the m^{th} root of the first order Bessel function of the first kind.

End corrections for side branches are difficult to determine analytically but have been obtained through the boundary element method by Ji³ as follows:

$$l_{0SB} = a \begin{cases} 0.8216 - 0.0644\xi - 0.694\xi^2 & \xi \leq 0.4 \\ 0.9326 - 0.6196\xi & \xi > 0.4 \end{cases} \quad (3)$$

where a is the radius of the neck and ξ is the ratio between the neck diameter and the side branch diameter. This correction can be added to the length over which the impedance is translated.

Thermo-viscous losses occur at the boundaries of a duct (α_w) and must be accounted for to obtain an accurate model. These losses can be accounted for by defining a complex wave number given by Pierce⁴:

$$\tilde{k} = \frac{\omega}{c} + \alpha_w - j\alpha_w \quad (4)$$

$$\alpha_w = \frac{1}{ac} \left(\frac{\eta\omega}{2\rho_0}\right)^{\frac{1}{2}} \left(1 + \frac{\gamma-1}{\sqrt{\text{Pr}}}\right). \quad (5)$$

where a is the radius of the tube, η is the coefficient of shear viscosity of air, γ is the ratio of specific heats, and Pr is the Prandtl number. The complex wave number can then be used instead of the traditional k in all the preceding equations to incorporate damping.

2.2 ELEMENT-BY-ELEMENT METHOD

One simplification that can be made to the previous method is to consider the impedance of individual elements in isolation. Instead of translating the impedance over an entire system, one

component of the resonator can be viewed separately and added in series or parallel with another component.

For a Helmholtz resonator, a cavity can be considered to have an infinite impedance at one end. Using Eqn. (1) with an infinite termination impedance, the equation collapses to:

$$Z_{A0} = -\frac{j\rho_0 c}{S} \cot(kL). \quad (6)$$

If the neck of a resonator is viewed in isolation, the impedance at the termination is zero and Eqn. (1) collapses to:

$$Z_{A0} = \frac{j\rho_0 c}{S} \tan(kL). \quad (7)$$

Furthermore, a simpler empirical formula for end corrections at a discontinuity can be used to decrease computation time. Bies and Hansen⁵ give the following end correction:

$$l_{0D} = 0.82a(1 - 1.33\xi), \quad (8)$$

where a is the radius of the neck and ξ is the ratio between the diameter of the neck and the diameter of the cavity.

An alternative method for calculating the damping is used that does not rely on complex wavenumbers. According to Morse and Ingard⁶, the acoustic resistance can be calculated as follows:

$$R = \frac{\rho_0 c k t D L}{2S^2} \left[1 + (\gamma - 1) \sqrt{\frac{5}{3\gamma}} \right] \quad (9)$$

where D is the internal duct cross-sectional perimeter and t is the viscous boundary layer thickness given by:

$$t = \sqrt{\frac{2\mu}{\rho\omega}}. \quad (10)$$

In the preceding equation, μ is the dynamic viscosity of air.

By adding these elements in series and parallel, the wave effects that occur within each component will be preserved, but they will not extend throughout the entire model.

2.3 LUMPED ELEMENT METHOD

The previous method can be simplified even further by assuming that only wavelengths much larger than the dimensions of the pipe will propagate in the system (i.e., $kL \ll 1$). With this assumption, equations (6) and (7) can be approximated using the first term in their respective Taylor series expansions as follows:

$$Z_{A0} \approx -\frac{j\rho_0 c}{S} \frac{1}{kL} = \frac{1}{j\omega V / \rho_0 c^2} \quad (10)$$

and

$$Z_{A0} \approx \frac{j\rho_0 c}{S} kL = j\omega \frac{\rho_0 l}{S}. \quad (11)$$

The expressions given in Eqns. (10) and (11) are the classical formulations for an acoustic compliance and an acoustic mass. Using these elements in series and parallel configurations with the end corrections and acoustic resistance given in the previous section, one can compute the response of an acoustic resonator or array of acoustic resonators.

3 RESULTS

In order to validate the three methods, an arbitrary resonator array was designed and fabricated. A schematic with pertinent labels is provided in Fig. 3 and the actual array is shown in Fig. 4.

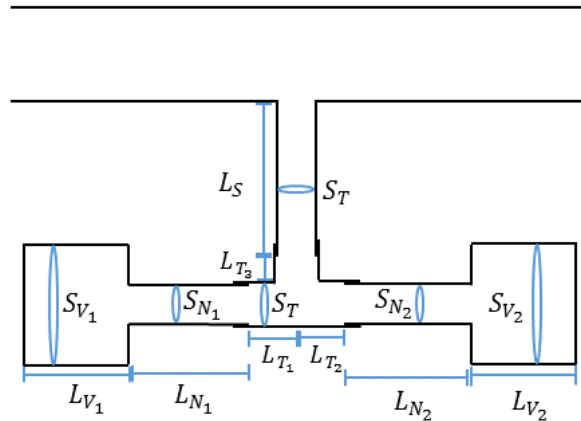


Fig. 3 - Schematic of the resonator array under test.

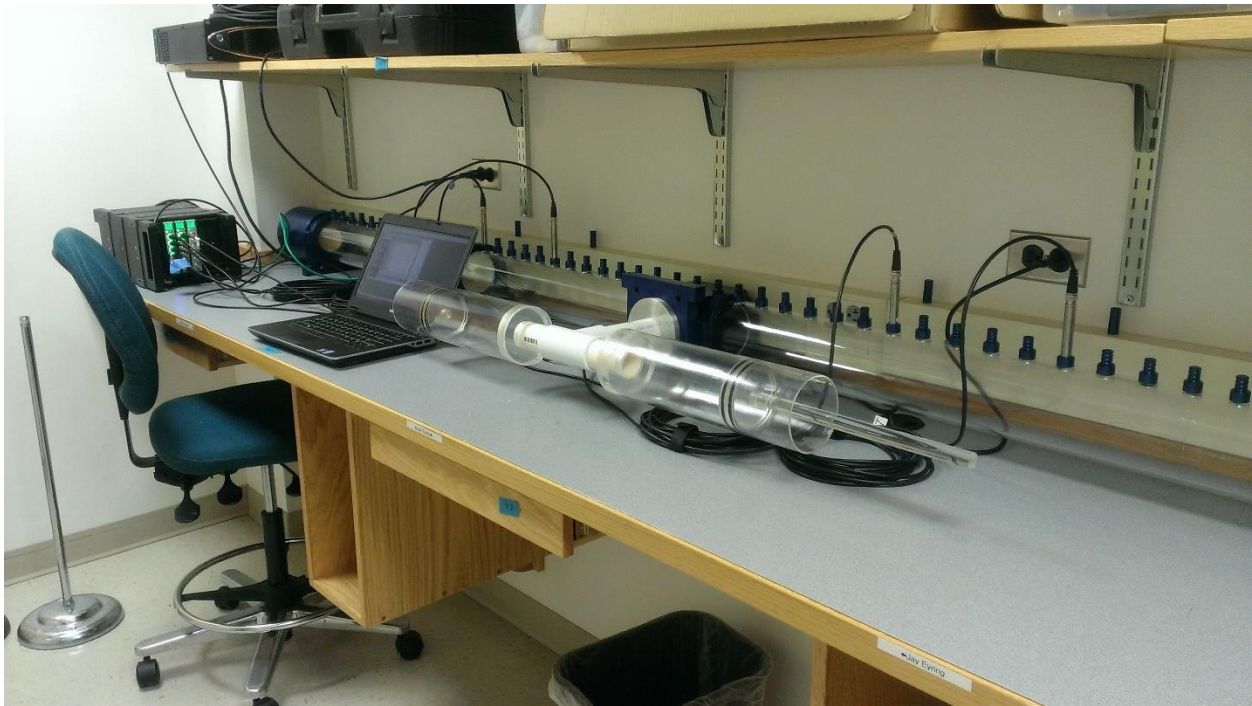


Fig. 4 - Setup of the actual resonator array under test.

Using the impedance translation method, an equivalent circuit was designed for the array of resonators. The resulting equivalent circuit for the configuration is shown in Fig. 5.

The results were compared with transmission loss data collected using the two microphone method⁷⁻⁸. The results for each of these methods is shown in Fig. 6.

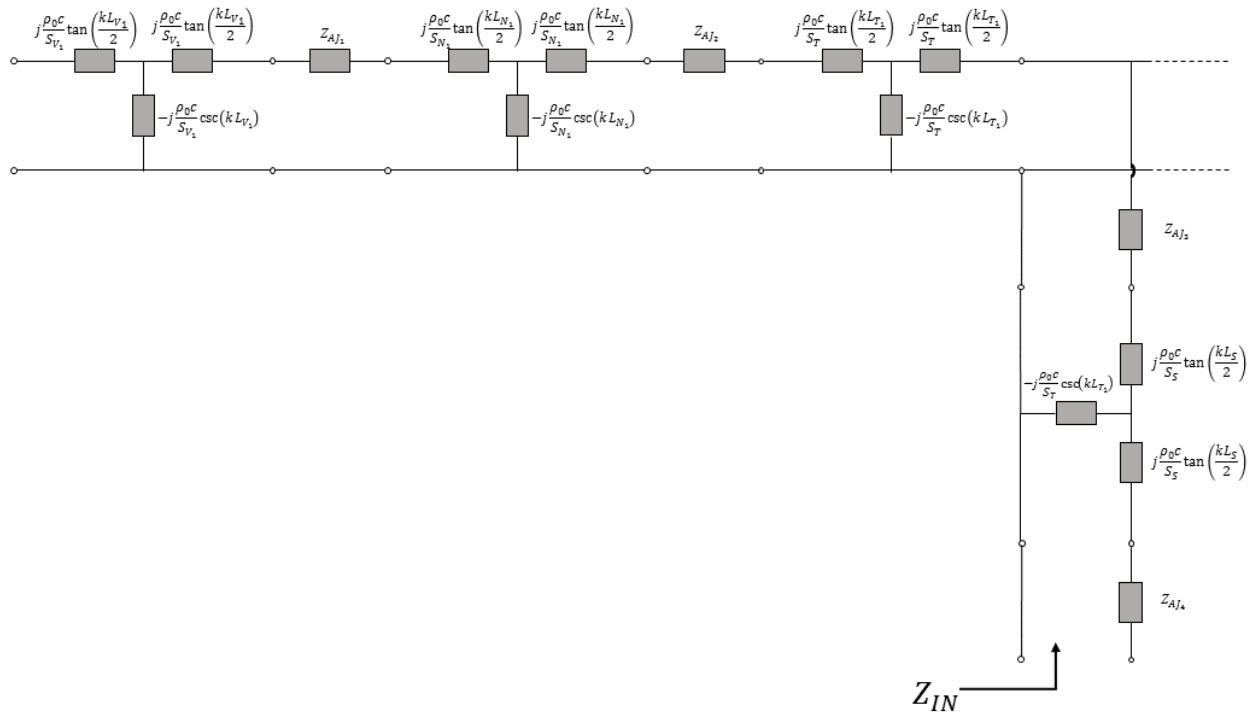


Fig. 5 - Equivalent circuit of the resonator array. The dots to the right of the circuit represent the branch leading to the second resonator. The branch that is not pictured is a mirror image of the first resonator branch.

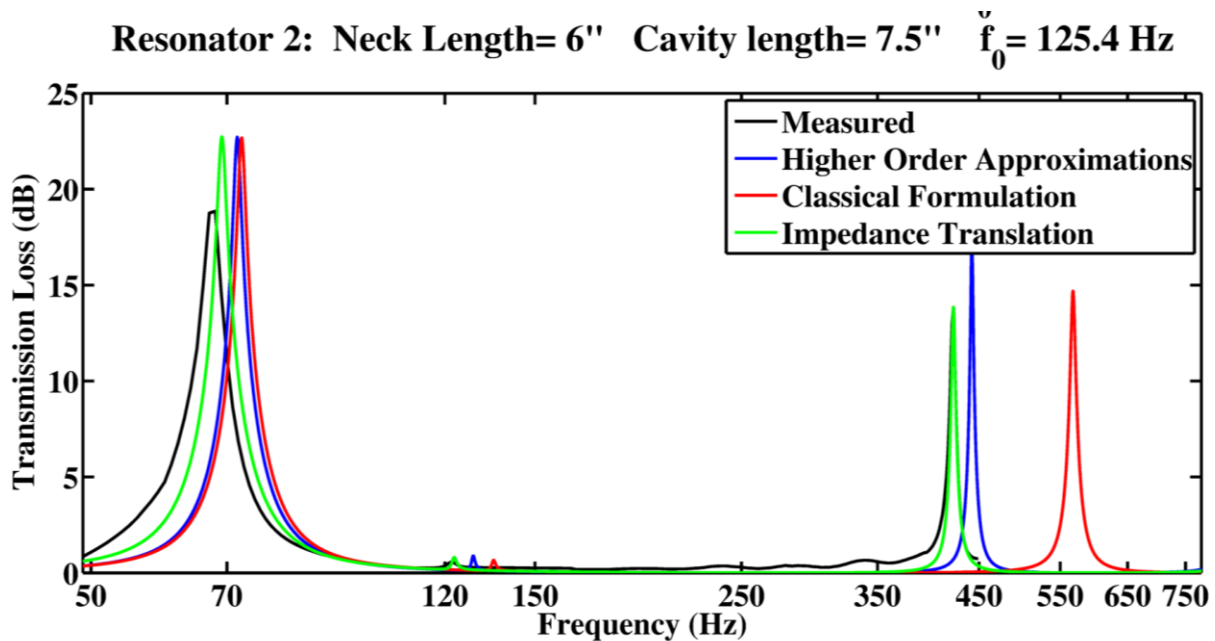


Fig. 6 - Comparison of transmission loss for measured and modeled data.

4 DISCUSSION AND CONCLUSIONS

First, the measured results – taken with 1 Hz resolution – show a primary peak between 67 and 68 Hz. Individually, the two parallel resonators have resonances at 140.6 Hz and 125.4 Hz. However, the configuration creates a much lower resonance than either of the resonators would produce in isolation. Although this result may be initially unexpected, all three models predict this frequency shift, which occurs because the two resonator impedances add in parallel. The equivalent circuit performs the best with a predicted resonance at 69.2 Hz. The element-by-element method predicts 71.7 Hz while the lumped element model predicts 72.7 Hz.

The small secondary peak at 122 Hz provides insight into how each model responds as frequency increases. The equivalent circuit predicts 122.8 Hz, but the other two models have increased error. The element-by-element method shows a peak at 128.7 Hz and the lumped element method predicts 135.4 Hz. As frequency increases, the approximation of $kL \ll 1$ starts to break down. The element-by-element method retains all terms in the trigonometric functions and therefore performs better than the lumped element method. However, since wave effects are not preserved between elements, both of these methods lose accuracy.

Finally, the large peak at 422.3 Hz is predicted very well by the equivalent circuit. However, the error in the other models has increased dramatically. The element-by-element method predicts a resonance at 442.2 Hz, while the lumped element model predicts a resonance at 568.1 Hz. The lack of wave effects and violation of the small kL approximation in these two models have led to significant error.

The results above show how each of these models may be used. If an engineering application requires only low frequency results, any of the models can provide adequate results. For applications where resonances lie within higher frequency bands, the element-by-element method may still provide accurate predictions. If secondary resonances in any frequency band are of interest to the engineer, the element-by-element and lumped element methods will fail to provide accurate results. In such cases, the impedance translation method should be applied where possible.

5 ACKNOWLEDGEMENTS

The authors would like to thank Caterpillar Inc. for funding and supporting this research. They would also like to thank Brigham Young University for the resources that have been made available for this research.

6 REFERENCES

1. M. Alster, "Improved calculation of resonant frequencies of Helmholtz resonators", *Journal of Sound and Vibration* **24**(1), 63-85, (1972).
2. F.C. Karal, "The analogous acoustical impedance for discontinuities and constrictions of circular cross section", *J. Acoust. Soc. Amer.*, **25**(2), 327-334, (1953).

3. Z. L. Ji, "Acoustic length correction of closed cylindrical side-branched tube." *Journal of Sound and Vibration* **283**(3-5), 1180-1186, (2005).
4. A. D. Pierce, *Acoustics: An introduction to its physical principles and applications*, Acoustical Society of America, (1994).
5. D. Bies and C. Hansen, *Engineering noise control: Theory and practice*, Unwin Hyman, London, (1988).
6. P. Morse and K. Ingard, *Theoretical acoustics*, McGraw-Hill, New York, (1968).
7. J. Y. Chung, and D. A. Blaser "Transfer function method of measuring in-duct acoustics properties I. Theory", *J. Acoust. Soc. Amer.*, **68**(3), 907-913, (1980).
8. J. Y. Chung, and D. A. Blaser, "Transfer function method of measuring in-duct acoustics properties II. Experiment", *J. Acoust. Soc. Amer.*, **68**(3), 914-921, (1980).